Application of the finite-element-discrete-model method for calculating resonance properties

G. A. Gallup*

Department of Physics and Astronomy, University of Nebraska-Lincoln, Lincoln, Nebraska 68588-0299, USA

(Received 6 April 2011; published 6 July 2011)

A enhanced procedure implementing the finite-element-discrete-model method [R. K. Nesbet, Phys. Rev. A **24**,1184 (1981)] for determining atomic or molecular shape resonances and widths is described. The present procedure includes an approximation for the static exchange plus polarization model involving Möller-Plesset perturbation theory. Applications to Mg, N_2, CH_2O, and uracil are described. Compared with experiment, the results for Mg are within 5 meV for the resonance position and 75 meV for the width. The vertical geometry results for N_2 and CH_2O compare well with experiment insofar as can be determined in the presence of nuclear motion complications. Uracil is calculated as an example where the large dipole moment (4.8 D) has an impact on threshold properties and possible dipole bound states.

DOI: 10.1103/PhysRevA.84.012701 PACS number(s): 34.80.Bm, 34.80.Ht

I. INTRODUCTION

Recently, increased experimental and theoretical interest in dissociative electron attachment (DEA) has occurred, induced by the experimental discovery of DNA strand breaking by low-energy electrons [1,2]. The theoretical treatment of DEA and related molecular processes is normally based upon the Born adiabatic theory [3,4] of nuclear motion, which depends upon accurate knowledge of the electronic properties of the molecule. Principally, these are fixed nucleus positions and lifetimes of resonance states and are usually determined with some version of the Fano-Feshbach [5–8] theory of the lifetimes of transient states. Domcke [9] has reviewed this subject with special emphasis on electron-molecule collisions. The current paper revisits a technique for approximating solutions to the Fano-Feshbach procedure that, apparently, has lain dormant for some years. We apply it to electronic resonances in Mg, N_2, formaldehyde, and uracil to display some of its characteristics.

Its earliest applications were associated with the Stieltjes moment theory that was discussed and applied to the problem of calculating transition moments in quantum mechanical systems [10,11]. About the same time Hazi [12,13] and Hazi *et al.* [14,15] utilized some of these ideas to calculate the lifetime of electronic resonances in a number of simple systems. Nesbet [16] continued the development, but referred to it as a finite-element-discrete-model (FEDM) method, noting that smoothing by means of the Stieltjes moment theory is not relevant to its application. Smoothing is an important issue and is discussed more fully below. We shall continue to use the FEDM appellation..

Briefly, the FEDM method involves using a set of discrete, normalizable functions to approximately represent the electronic continuum in a conventional Fano-Feshbach [5–8] treatment of atomic or molecular resonances. With it one obtains the complex energy shift, $\Delta(E) - i\Gamma(E)/2$, characteristic of the theory and within the limitations of the various approximations.

One of the requirements of the Fano-Feshbach approach is the construction of a function representing the quasi-bound state (QBS) corresponding to the resonance. In an exact calculation, the details of this function do not affect the outcome. When approximations are required, however, the details matter. We have found that using a properly constrained basis provides an appropriate QBS. In this paper we discuss the construction of bases for the FEDM method, and finally applications to several systems are given.

In assessing a theory such as this, it is useful, for vetting, to have experimental results to compare with. It must be admitted that this is difficult, since our principal interest is in molecular shape resonances, where Franck-Condon and other nuclear motion effects can obscure the purely electronic part of the phenomenon. This does not happen with single atoms, and thus our first application in Sec. III treats comparisons with the ^2P shape resonance in Mg, which, among smaller nonrelativistic systems, arguably has the best experimental values for a shape resonance yielding both energy and width values. Results are given for further applications to the diatomic molecule N_2, where in Sec. III B we comment further on effects of nuclear motion. In addition the polyatomic molecules formaldehyde, $CH_2{=}O$, and uracil, $C_4H_4N_2O_2$, are treated

II. THEORY

A. The finite-element-discrete-model method

The Fano-Feshbach theory of the lifetime of a decaying state is closely related to the "Golden Rule" [17–19] and is given by

$$\Gamma(E) = 2\pi |\langle \phi | H | \psi_P(E) \rangle|^2, \tag{1}$$

where ϕ is the function corresponding to the decaying state and defines the projectors

$$Q = |\phi\rangle\langle\phi| \tag{2}$$

and

$$P = I - Q. \tag{3}$$

In addition, for the version of the Golden Rule shown in Eq. (1), $\psi_P(E)$ must be energy normalized and have the density

*ggallup1@unl.edu;[http://www.unl.edu/ggallup/]

of states factor folded into it. $\psi_P(E)$ must also satisfy the equations

$$(PHP - E)\psi_P(E) = 0, \tag{4}$$

$$\langle\psi_P(E)|\psi_P(E')\rangle = \delta(E - E'), \tag{5}$$

and

$$\int dE|\psi_P(E)\rangle\langle\psi_P(E)| = P. \tag{6}$$

One also defines $\psi(E)$, which is the total continuum wave function corresponding to the Hamiltonian and satisfies

$$(H - E)\psi(E) = 0, \tag{7}$$

$$\langle\psi(E)|\psi(E')\rangle = \delta(E - E'), \tag{8}$$

and also

$$\int dE|\psi(E)\rangle\langle\psi(E)| = I. \tag{9}$$

When translating these expressions into the FEDM approximation, it appears most convenient to deal with the cumulated function

$$F(E) = \int_0^E \Gamma(E')\, dE'. \tag{10}$$

The FEDM method involves approximating the exact cumulative function at the energies, E_n, with the expression

$$F(E_n) \approx F_n \tag{11}$$

$$= 2\pi \sum_{i=0}^{n} |V(E_i)|^2 \tag{12}$$

$$= 2\pi \sum_{i=0}^{n} \left|\frac{V(E_i)}{\sqrt{d_i}}\right|^2 d_i, \tag{13}$$

where

$$V(E_i) = \langle\phi|H|u_i\rangle, \tag{14}$$

$$d_i = \tfrac{1}{2}(\langle u_{i+1}|H|u_{i+1}\rangle - \langle u_{i-1}|H|u_{i-1}\rangle), \tag{15}$$

and u_i is one of a set of L^2 functions that are orthogonal to ϕ. We shall call the u_i pseudo-continuum (PC) functions. The interpretation of Eq. (13) is clear, representing a trapezoid rule integration approximation. The necessary energy density normalization is produced by the $\sqrt{d_i}$ in the denominator.

As pointed out by Nesbet, the FEDM method is actually an *ansatz* based upon Eq. (12), with the expectation that the approximation is improved as the E_n become closer together. There has apparently been no rigorous proof that a PC set satisfying these conditions can exist. The PC functions we use in practice are described in Sec. II B and consist of a set of Gaussian functions that do not necessarily have the correct limiting properties guaranteeing that Eq. (12) becomes more exact as the energy density of the discrete functions increases. The idea is nevertheless intuitively appealing.

B. The pseudo-continuum functions

The PC functions are symmetry-projected and spin-projected Slater determinant (SPSD) functions based upon neutral molecule states with added orbitals for the extra electron. An added orbital is one of a series of Gaussian functions,

$$u_{ilm}(\vec{r}) = N_i Y_{lm} r^l \exp(-\zeta_i \vec{r}^{\,2}), \tag{16}$$

where the Y_{lm} in our application are normally "tensorial" (rather than spherical) harmonics, and the ζ_i coefficients for a given l-m pair are in a geometric progression between appropriate limits, that is, the ζ_i for different m and the same l may differ. The constant ratio, ζ_{i+1}/ζ_i, between adjacent exponential coefficients cannot normally be $\lessapprox 1.6$ without causing numerical difficulties with calculations. It has also been found that runs of between 15 and 20 functions for each l-m pair appear satisfactory for our purpose. Where appropriate, two or more overlapping runs may be used.

C. Description of the computational pathway

1. A not too flexible (see Sec. II D) atomic orbital basis is chosen, and the standard one- and two-electron integrals are calculated for the neutral molecule equilibrium geometry. All our applications will be for *vertical* geometry processes, and this geometry will not change throughout the application of the FEDM procedure. With this basis conventional restricted closed-shell Hartree-Fock (RHF) and restricted open-shell Hartree-Fock (ROHF) treatments of the neutral molecule [20] and its negative ion are performed, producing two sets of orbitals that we will label MO_n and MO_i, respectively.

2. Integrals are evaluated for the atomic orbitals of Step 1. augmented with the pseudo-continuum orbital (PCOs) to be used, and these are subjected to an orbital transformation involving selections from the MO_n set, from the MO_i set, and from unmodified PCOs. At this stage the MO_n and MO_i sets are internally orthonormal, and the PCO set is normalized but not orthogonal.

3. The integrals from Step 2 are combined into two sets of "$(n + 1)$"-electron configurations.

Set 1. One or more SPSDs are constructed from configurations built from the MO_i set of Step 1, i.e., orbitals from the ion calculation.

Set 2. Configurations are constructed consisting of the neutral molecule orbitals and one each of the PCOs.

This combined set produces Hamiltonian and overlap matrices corresponding to a spatial symmetry restricted SPSD basis of the configurations. This will include all of the possible spin couplings and is accomplished with a non-orthogonal-orbital matrix element generator [21].

4. At this stage the H and S matrices both have the block structure

$$\begin{bmatrix} A_X & B_X^\dagger \\ B_X & C_X \end{bmatrix},$$

where the A_X blocks are associated with the QBS states included, the C_X blocks are associated with the PCO states, and $X = H$ or S.

5. The A_H and C_H blocks of H are now diagonalized, and the corresponding A_S and C_S blocks become identity matrices.

6. The C rows and columns are subjected to a transformation that converts those columns of B_X corresponding to final

QBSs to zero. That is, the QBSs are projected out of the PCO eigenstates.

7. Now the C_H-C_S system is rediagonalized, and the necessary matrix elements for use in Eqs. (12), (14), and (15) are in the appropriate columns of B_H and the diagonal elements of C_H.

1. The fitting problem

Once the discrete values of the $F(E)$ function are available, they must be converted to the smooth functions, $\Gamma(E)$ and $\Delta(E)$. As indicated in Sec. I the smoothing of the discrete values is a concern with the FEDM method. Different previous workers have used different schemes. We have found useful a procedure utilizing the functions proposed by Mündel and Domcke [22] that are outlined in the Appendix. In general, a linear combination of the width functions, Eq. (A1), is used to approximate $\Gamma(E)$,

$$\Gamma(E) = \sum_k A_k (E/B_k)^{\alpha_k} \exp(-E/B_k), \tag{17}$$

and the A_k, B_k, and α_k are adjusted by a least-squares procedure to minimize the difference between the corresponding cumulated function,

$$F^{ls}(E) = \sum_k A_k B_k \gamma(\alpha_k + 1, E/B_k), \tag{18}$$

and the discrete values from Eq. (12). Thus we minimize the variance

$$\mathcal{V} = \sum_n \frac{[F_n - F^{ls}(E_n)]^2}{w_n}, \tag{19}$$

where w_n is a weighting denominator for the various points. Several different choices for the weighting denominators have been tested and $w_n = F_n^2$ appears the most satisfactory. The F_n values can vary over two to five orders of magnitude, and this choice results in minimizing the sum of squares of the relative errors. The "downhill simplex" method of Nelder and Mead [23] for minimization has proved completely satisfactory.

As stated above, the smoothing of the F_n values has always been an issue with the FEDM method. Most of the earlier studies involved cases where the QBS was well represented by one partial wave. In our cases several lm waves may be important at once. This can produce what appears to be a small interference effect. We show an example of this in Fig. 1, which displays F_n versus E_n data on a log-log graph. The QBS here corresponds to the C=O antibonding orbital of formaldehyde and consists of a sum of p and d waves. A definite oscillatory behavior is evident at low energy, and the graph also shows a typical fitted F^{ls} using just one term in Eq. (18).

D. GTO basis flexibility

Section II C contains the assertion that the Gaussian-type orbital bases used to represent the QBS must be "not too flexible." This imprecise terminology reflects the well-known phenomenon of variational collapse when temporary (decaying) negative ions are described using excessively diffuse basis sets. It also reflects the imprecise definition of the QBS within the Fano-Feshbach theory at the outset. Froelich and Brandäs [24] have suggested a definition of an optimal QBS, but it involves matrix elements of $\langle b|(H-E)^2|b\rangle$ that present severe difficulties with many-electron systems. The R-matrix method indirectly solves the problem by (for example) using the Bloch operator [25] to prevent variational collapse. The present technique uses the constraints inherent in the standard GTO basis set, 6-31G(d), for most calculations. The lower energy lowest unoccupied molecular orbitals ($\leqslant$5 eV) provide our ingredients to construct the QBSs needed for shape resonances. The higher energy lowest unoccupied molecular orbitals are less satisfactory.

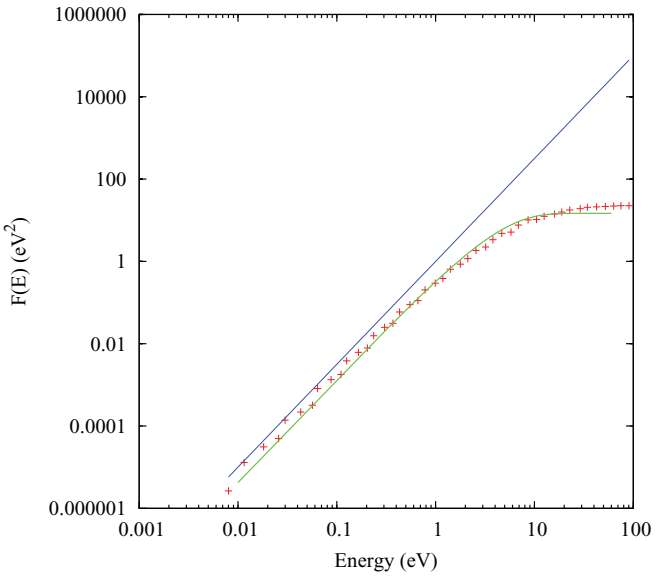

FIG. 1. (Color online) A fit of the F_n values for a QBS corresponding to the C=O antibonding π orbital of formaldehyde at equilibrium geometry. The red crosses are the F_n points, the curved green line is the F^{ls} curve for one term, and the straight blue line shows the expected threshold slope of $E^{2.43}$ (see text). It is seen that the best-fit threshold slope is very close to the ideal.

III. APPLICATIONS

A. The *p*-wave resonance in Mg

As stated before, the experimental results for the ^2P shape resonance in the Mg atom are the best known among the lighter atoms. It therefore provides a good testing ground for the current method, as it has none of the complications due to nuclear motion present in molecules.

The ^2P resonance in Mg has been measured by Burrow and Comer [26] and again by Burrow *et al.* [27]. In the earlier work, focusing on the lowest energy range, the values reported for the resonance position are $E_r = 0.15$ eV and width $\Gamma(E_r) = 0.16$ eV.

We use a conventional 6-31G(d) Gaussian basis for the Mg core. The $F(E)$ function was calculated using 15 PCOs ranging in kinetic energy from 15.0 to $\approx$0.0052 eV, and, following the computational path outlined in Sec. II C the values are shown in Table I.

The analytic functions of the Appendix were used for fitting $F(E)$ and associated quantities from the data in Table I with the value of α constrained to be 3/2. The results are shown in Fig. 2, which shows plots of the resulting $\Gamma(E)$, $\Delta(E)$, and $E -$

TABLE I. Calculated E and $F(E)$ values.

E_n (eV)	$F(E_n)$ (eV^2)
1.2544×10^{-2}	$1.220\,023\times10^{-4}$
3.0995×10^{-2}	$8.438\,343\times10^{-4}$
6.3631×10^{-2}	$4.015\,035\times10^{-3}$
1.2028×10^{-1}	$1.575\,346\times10^{-2}$
2.1900×10^{-1}	$5.443\,744\times10^{-2}$
3.9342×10^{-1}	$1.699\,031\times10^{-1}$
7.0889×10^{-1}	$4.862\,681\times10^{-1}$
1.2969	1.246 161
2.4142	2.570 280
4.4778	3.509 513
7.2753	3.729 412
9.6424	4.216 745
1.5014	5.183 965
2.8813	5.884196[a]

[a]There are only 14 values because of the averaging procedure of Eqs. (12) and (15).

$E_b - \Delta(E)$ functions. The last of these shows a graphical solution for the resonance energy E_r in terms of the QBS energy E_b and the real part of the energy shift $\Delta(E)$. In this case the E_b value is determined from the sum of the self-consistent field Δ(SCF) (1.10273 eV) energies of Step 1 and the MP2 value for the polarization interaction (−0.16935 eV), which gives 0.93338 eV.

For E_r the results of this calculation give 0.159 eV, and Burrow and Comer [26] give 0.15 eV, which is quite satisfactory agreement (see also Ref. [13]). The situation with the width comparison is more difficult. The cross section is very unlikely to resemble a simple Lorentz function, since from Fig. 2 we see that Γ is changing rapidly in the vicinity of E_r, and the $1/E$ factor in the cross section is also changing rapidly at this point. Setting up a model calculation involving the calculated resonance parameters as well as an orthogonality

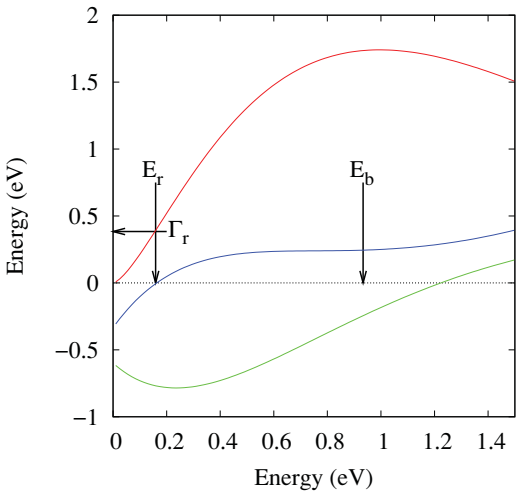

FIG. 2. (Color online) $\Gamma(E)$ (red, upper curve), $\Delta(E)$ (green, lower curve), and $E - E_b - \Delta(E)$ (blue, middle curve) from the FEDM calculation of Mg. The curves may also be identified by their behaviors. $\Gamma(E)$ is necessarily positive, and $E - E_b - \Delta(E)$ is zero at E_r. The arrows also show various values graphically.

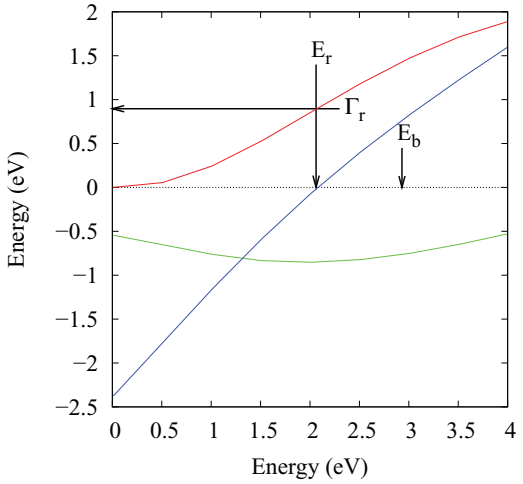

FIG. 3. (Color online) FEDM results for N_2. The representational details are the same as in the caption of Fig. 2.

phase shift (see Ref. [9]) and a model p-wave cross section, we can find the second derivative. The points where this is zero give our calculated dip-to-peak energy separation of 0.12 eV, somewhat smaller than the electron transmission spectroscopy (ETS) measurement, but still with good agreement. Burrow *et al.* [27] also measured the Mg resonance by the electron transmission method, where it is seen that the resonance peak rides on a slanted but fairly straight slope. In addition, the orthogonality phase shift is normally proportional to $E^{l+1/2}$ and small. Neither should contribute strongly to the second derivative, so our dip-to-peak energy separation should not be strongly affected by their neglect.

The Mg calculations were also carried out with 20 PC functions that spanned a similar kinetic energy range. The final results were virtually indistinguishable from the above results with 15 functions.

B. N_2

Following the same procedure, we obtained for N_2 the results shown in Fig. 3, with calculated values of $E_r = 2.05$ eV and $\Gamma(E_r) = 0.859$ eV. Th ΔSCF energy is 3.774 eV, which is reduced to $E_b = 2.931$ eV by the MP2 polarization correction.

The shape resonance in N_2 was first observed by Ramsauer and Kollath [28] in 1931 and is probably the most studied, both experimentally and theoretically, of any shape resonance in molecules. The most modern measurements were obtained by Golden [29], Ehrhardt and Willmann [30], and the latest by Kennerly [31]. We again emphasize that we are calculating the properties of the vertical process, and, examining Kennerly's tabular data for the cross section, one sees that there are two nearly equal strength peaks at 2.219 and 2.442 eV. If the actual vertical value is between these, as is expected by analogy with optical spectra, we see that our calculation gives an electronic resonance center that appears low by ≈0.25 eV. It should be noted that this criterion may not be useful. Examination of Eqs. (4)–(8) through (4)–(11) of Ref. [9] and references therein shows that, theoretically, transitions between nuclear motion states, at least one of which is associated with a

TABLE II. Populations of different spherical l spaces in the singly occupied molecular orbital (SOMO) of the QBS for CH_2O. The expansion point is the center of mass and the C_{2v} and spherical z axes coincide.

l	Population
0	0.000 000 00
1	0.251 078 37
2	0.571 465 63
3	0.064 289 48
4	0.056 251 44
5	0.019 967 83
6	0.011 006 41

decaying electronic state, are governed by Franck-Condon-like integrals modified by the R-dependent lifetime amplitude of the electronic state. Thus, we can only say that the present calculated electronic resonance position is certainly in the neighborhood of the actual experimental value.

Schulz [32] has published an extensive review of the subject, and, using his measurements, Birtwistle and Herzenberg [33] have given a theoretical analysis of the resonance profile and vibrational excitation. Their results gave 0.57 ± 0.02 eV for the vertical Γ, somewhat smaller than our value above.

C. Formaldehyde, CH_2O

Formaldehyde is a molecule with a π^* resonance [34,35] that has lower symmetry than that in N_2. CH_2O also possesses an electric dipole moment of 2.85 D, considerably above the fixed nucleus critical value of 1.6238 . . . D. For such a value one expects the s-wave (strictly speaking, a_1-wave) $\Gamma(E \to 0) > 0$. The π^* resonance is, however, associated with $|m| = 1$, and a moment of $\geqslant 9.631\ldots$ D is required before a finite threshold behavior is expected.

Table II gives a population analysis of the QBS SOMO and shows that it is over 50% $l = 2$ and approximately a quarter $l = 1$. Components for $l > 2$ comprise the remainder. A further discussion for the $m = 0$ case of supercritical dipole moment molecules is in Sec. III D.

The results for the cumulated function have been shown in Fig. 1, where we see that $F(E \to 0) \propto E^{2.43}$. Thus, $\Gamma(E \to 0) \propto E^{1.43}$, consistent with the dipole moment and the populations. Figure 4 shows $\gamma(E)$, $\Delta(E)$, and $E - \Delta(E) - E_b$ curves for CH_2O.

The present FEDM values for the electronic part of the resonance are $E_r = 0.682$ eV and $\Gamma(E_r) = 0.429$ eV. The ΔSCF value is 2.302 eV and this is reduced to 1.454 eV by the polarization correction. The experimental results show several resonance peaks associated with molecular vibrations. In electron volts the energies of the first two are given by Burrow and Michejda [34] as 0.65 ± 0.05 and 0.86, by van Veen *et al.* [36] as 0.66 and 0.86, and by Benoit and Abouaf [35] as 0.67 and 0.89, all in good agreement. No direct experimental value for Γ has been found, but, from their vibrational excitation measurements, Benoit and Abouf argue that it is neither very much larger nor very much smaller than 0.216 eV, the ν_2 (C=O stretch) vibrational frequency of the neutral molecule. The Franck-Condon factors here are

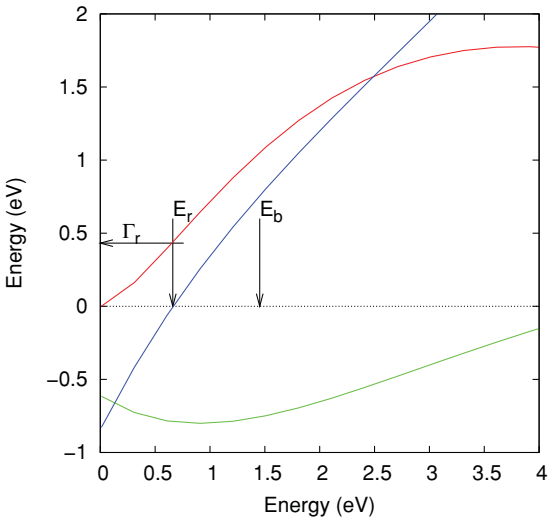

FIG. 4. (Color online) The FEDM results for CH_2O. The representational details are the same as in the caption of Fig. 2.

subject to the same complications discussed in Sec. III B and the FEDM procedure yields satisfactory results.

D. Uracil and σ^* resonances

Uracil is a biologically important molecule that appears in the coding for RNA. It is a heterocyclic six-membered ring compound, and we are interested particularly in the shape resonance associated with the N_1–H (there being two N atoms in the ring, N_1 and N_2) antibonding orbital. This bond is ruptured in production of the $(M\text{-}H)^-$ negative ion at low energies. The electric dipole moment is fairly large at ≈4.8 D and is directed only about 8° from the N_1–H bond direction in the neutral molecule.

Recent measurements show π^* shape resonances [37]. These are expected to behave similarly to the π resonance in formaldehyde and have a zero energy threshold proportional to $E^{1.26}$ with this dipole moment and $|m| = 1$. Uracil also

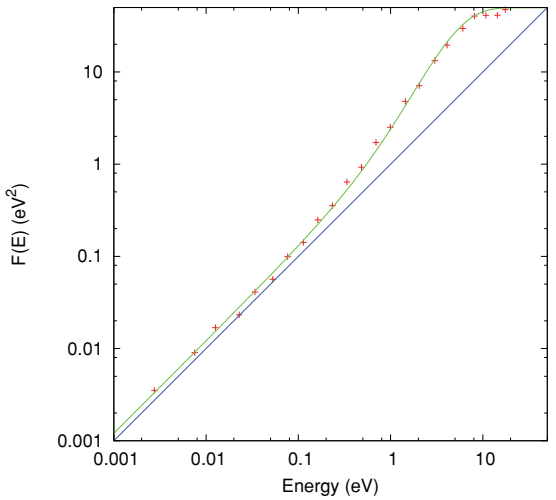

FIG. 5. (Color online) Uracil $F(E)$ function fit. See Fig. 1 caption for represntational details. The solid straight line shows the expected slope of the E vs E line.

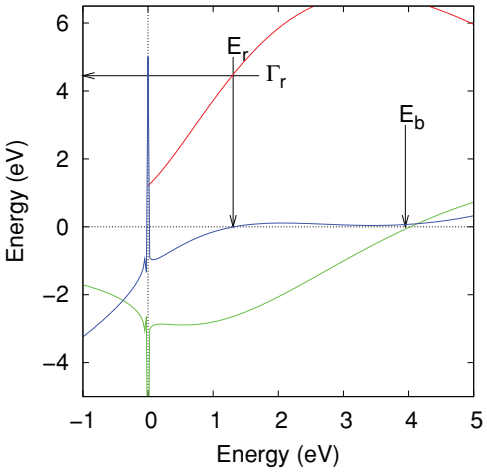

FIG. 6. (Color online) FEDM results for uracil. The representational details are the same as in the caption of Fig. 2.

undergoes DEA to form an $(M\text{-}H)^-$ by loss of the H atom attached to N_1, and the cross section was determined by Aflatooni and Burrow [38]. The FEDM was applied to DEA to uracil by Gallup and Fabrikant [39]. Here, the application of tha FEDM to the N_1-H σ^* "resonance" for the neutral molecule equilibrium geometry is discussed in detail.

Proceeding as before, with a set of 15 s functions and 15 p_σ functions, we obtain the results of Fig. 5, which shows the $F(E)$ function and the data points on a log-log graph where it is seen that the threshold is finite since $F(E) \propto E$. It is well known that the point dipole potential predicts in the fixed nucleus approximation (FNA) an infinite number of dipole bound states (DBSs) when its magnitude is above the critical value of 1.6239 . . . D. Fabrikant [41,42] has also shown that the threshold law becomes finite at this value. More recently the present author [43] has shown that a physical dipole model shows similar but not sharp behavior. The physical dipole system has wave functions regular at the origin and at the point charges. Thus our FEDM correctly produces a $\Gamma(E)$ function emulating this threshold behavior.

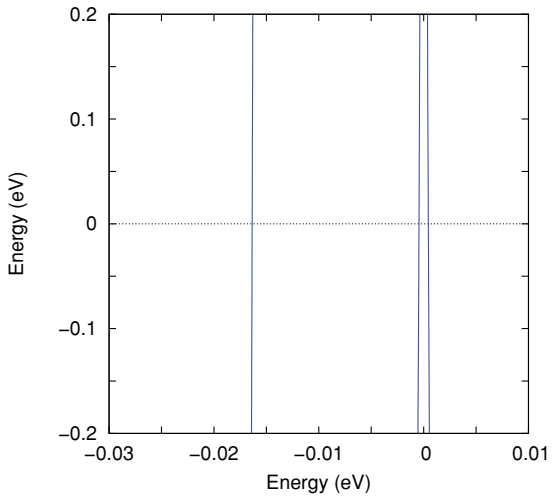

FIG. 7. (Color online) A blown-up view of a region near the origin of Fig. 6. The crossings are at −36, −0.59, and 0.29 meV.

The finite threshold results in a weak logarithmic singularity in the real energy shift function at $E = 0$ are shown in Fig. 6. We have altogether (in this approximation!) four roots of the equation, $E - \Delta(E) - E_b = 0$, in the range of the abscissa. The upper root predicts that there is a very broad $\Gamma(E_{\rm res})\approx 5$ eV resonance at 2.0 eV that might well be obscured in total scattering eigenphases or in experiments. As seen in Ref. [39] the energy of the root falls rapidly as the N_1–H bond distance is lengthened from the equilibrium neutral value.

The nature of the roots near zero is obscured in Fig. 6, but a blown-up section near the origin in Fig. 7 shows the three of them, with the lowest of the four at −0.036 eV. This reflects the presence of a DBS, which was observed at 0.093 ± 0.007 eV experimentally by Hendricks *et al.* [40]. The discrepancy here is due at least partly to our unrelaxed geometry. Our basis would be unable to produce any higher DBSs, the expected natures of which are shown in Ref. [43].

The two roots of $E - \Delta(E) - E_b = 0$ very near $E = 0$ are a consequence of the finite threshold. The implications of these are discussed in terms of S-matrix poles by Domcke [9] and are at least partly responsible for the large cross sections near zero energy found in dipolar molecules.

ACKNOWLEDGMENTS

The author sincerely thanks Professors P. D. Burrow and I. I. Fabrikant for very useful discussions and suggestions and the Department of Physics and Astronomy for their support.

APPENDIX: $F(E)$, $\Gamma(E)$, AND $\Delta(E)$ FUNCTIONS

For our fitting-smoothing functions we need two sorts depending upon the dipole moment of the molecule being treated. When the dipole moment is below the critical value, we use a slightly modified version of the forms given by Mündel and Domcke [22]. The primary function Γ is

$$\Gamma(E) = A(E/B)^\alpha \exp(-E/B), \tag{A1}$$

where A and B are parameters with energy units and α will many times be $l + 1/2$. $F(E)$, the cumulated function, is

$$F(E) = \int_0^E \Gamma(E')dE', \tag{A2}$$

$$= AB\gamma(\alpha + 1, E/B), \tag{A3}$$

where $\gamma(\beta,x)$ is the partial Γ function with limit $\Gamma(\beta)$ as $x \to \infty$. Mündel and Domcke also give the corresponding energy shift function

$$\Delta(E) = \frac{1}{2\pi}\int_0^\infty \frac{\Gamma(E')dE'}{E - E'} \tag{A4}$$

$$= \frac{\Gamma(E)}{2\pi}\left[\frac{\pi}{\tan(\alpha\pi)} - \Gamma(\alpha)(E/B)^{-\alpha}M(-\alpha, 1-\alpha, E/B)\right], \quad E > 0, \tag{A5}$$

and

$$= -\frac{A}{2\pi}\Gamma(\alpha+1)(-E/B)^{\alpha}\gamma(-\alpha,-E/B)\exp(-E/B), \quad E<0, \tag{A6}$$

where $M(a,b,x)$ is the Kummer version of the confluent hypergeometric function [44]. Thus the width function given in Eq. (A1) is very convenient since analytic expressions are available for both $F(E)$ and $\Delta(E)$.

For cases where the dipole moment is supercritical, the energy threshold value for $\Gamma(E)$ is not zero as given by the form of Eq. (A1), but will be nonzero [45]. For this case we use

$$\Gamma_d(E) = A\frac{1}{n!}\int_{E/B}^{\infty} y^n e^{-y}dy, \tag{A7}$$

$$= A\sum_{k=0}^{n}\frac{1}{k!}\left(\frac{E}{B}\right)^k \exp(-E/B), \tag{A8}$$

which has the desired behavior. The cumulated function is easily computed as

$$F_d(E) = AB\sum_{k=0}^{n} P(k+1,E/B), \tag{A9}$$

where P is the version of the partial Γ function given by

$$P(\alpha,z) = \frac{1}{\Gamma(\alpha)}\int_0^z y^{\alpha-1}e^{-z}dz. \tag{A10}$$

The energy shift function for this Γ form may be represented in terms of the exponential integral [44],

$$\Delta_d(E) = -\frac{A}{2\pi}\sum_{k=0}^{n}\frac{1}{k!}\left[e^{-E/B}J_{\lessgtr}\left(\frac{E}{B}\right)+\phi(k-1,E/B)\right], \tag{A11}$$

where

$$J_<(x) = E_1(-x), \quad x<0, \tag{A12}$$

$$J_>(x) = Ei(x), \quad x>0, \tag{A13}$$

$$\phi(-1,x) = 0, \tag{A14}$$

and

$$\phi(k,x) = 0!/x + 1!/x^2 + \cdots + k!/x^{(k+1)}. \tag{A15}$$

The principal effect of the n value among these dipole functions is an increase in the flatness of Γ near $E=0$ as n increases.

[1] B. Boudaïffa, P. Cloutier, D. Hunting, M. A. Huels, and L. Sanche, Science **287**, 1658 (2000).
[2] L. Sanche, Eur. Phys. J. D **35**, 367 (2005).
[3] M. Born and K. Huang *Dynamical Theory of Crystal Lattices* (Oxford University Press, London, 1951), Appendix VIII.
[4] M. Born, Gött. Nachr. Math. Phys. Kl. 1, (1951).
[5] U. Fano, Phys. Rev. **124**, 1866 (1961).
[6] H. Feshbach, Ann. Phys. (NY) **5**, 357 (1958).
[7] H. Feshbach, Ann. Phys. (NY) **19**, 287 (1962).
[8] H. Feshbach, Ann. Phys. (NY) **43**, 410 (1967).
[9] W. Domcke, Phys. Rep. **208**, 97 (1991).
[10] P. W. Langhoff, Int. J. Quantum Chem. **S8**, 347 (1974).
[11] C. T. Corcoran and P. W. Langhoff, J. Math. Phys. **18**, 651 (1977).
[12] A. U. Hazi, J. Phys. B **11**, L259 (1978).
[13] A. U. Hazi, in *Electron-Molecule and Photon-Molecule Collisions*, edited by T. Rescigno, V. McKoy, and B. Schneider (Plenum, New York, 1978).
[14] A. U. Hazi, T. N. Rescigno, and M. Kurilla, Phys. Rev. A **23**, 1089 (1981).
[15] A. U. Hazi, A. E. Orel, and T. N. Rescigno, Phys. Rev. A **23**, 918 (1981).
[16] R. K. Nesbet, Phys. Rev. A **24**, 1184 (1981).
[17] P. A. M. Dirac, Proc. R. Soc. London Ser. A **114**, 243 (1927).
[18] G. Wentzel, Z. Phys. **43**, 524 (1927).
[19] E. Fermi, *Nuclear Physics* (University of Chicago Press, Chicago, 1950).
[20] Our description here assumes that the neutral molecule is closed-shell. If this is not the case, modifications are required.
[21] G. A. Gallup, R. L. Vance, J. R. Collins, and J. M. Norbeck, Adv. Quantum Chem. **16**, 229 (1982).
[22] C. Mündel and W. Domcke, J. Phys. B **18**, 4491 (1985).
[23] J. A. Nelder and R. Mead, Comput. J. **7**, 308 (1965).
[24] P. Froelich and E. Brandäs Phys. Rev A **12**, 1 (1975).
[25] C. Bloch, Nucl. Phys. **4**, 503 (1957).
[26] P. D. Burrow and J. Comer, J. Phys. B **8**, L92 (1975).
[27] P. D. Burrow, J. A. Michejda, and J. Comer, J. Phys. B **9**, 3225 (1976).
[28] C. Ramsauer and R. Kollath, Ann. Phys. (Leipzig) **10**, 143 (1931).
[29] D. E. Golden, Phys. Rev. Lett. **17**, 847 (1966).
[30] H. Ehrhardt and K. Willmann, Z. Phys. **204**, 462 (1967).
[31] R. E. Kennerly, Phys. Rev. A **21**, 1876 (1980).
[32] G. J. Schulz, Rev. Mod. Phys. **45**, 423 (1973).
[33] D. T. Birtwistle and A. Herzenberg, J. Phys. B **4**, 53 (1971).
[34] P. D. Burrow and J. A. Michejda, Chem. Phys. Lett. **42**, 223 (1976).
[35] C. Benoit and R. Abouaf, Chem. Phys. Lett. **123**, 134 (1986).
[36] E. H. van Veen, W. L. van Dijk, and H. H. Brongersma, Chem. Phys. **16**, 337 (1976).
[37] A. M. Scheer, C. Silvernail, J. A. Belot, K. Aflatooni, G. A. Gallup, and P. D. Burrow, Chem. Phys. Lett. **411**, 46 (2005).
[38] K. Aflatooni and P. D. Burrow, Chem. Phys. Lett. **408**, 426 (2005).
[39] G. A. Gallup and I. I. Fabrikant, Phys. Rev. A **83**, 012706 (2011).
[40] J. H. Hendricks, S. A. Lyapustin, H. L. de Clercq, J. T. Snodgrass, and K. H. Bowen, J. Chem. Phys. **104**, 7788 (1996).
[41] I. I. Fabrikant, Sov. Phys. JETP **46**, 693 (1977).
[42] I. I. Fabrikant, J. Phys. B **11**, 3621 (1978).
[43] G. A. Gallup, Phys. Rev. A **80**, 012511 (2009).
[44] M. Abramowitz and I. A. Stegun, *Handbook of Mathematical Functions* (National Bureau of Standards, US Government Printing Office, Washington, DC, 1970).
[45] That is, it is a physical dipole; see [43].